Korean J. Chem. Eng., **21**(2), 477-487 (2004)

Separation Characteristics of Tetrapropylammoniumbromide Templating Silica/Alumina Composite Membrane in CO_2/N_2, CO_2/H_2 and CH_4/H_2 Systems

Jong-Ho Moon, Hyungwoong Ahn, Sang-Hoon Hyun* and Chang-Ha Lee†**

Department of Chemical Engineering, *Department of Ceramic Engineering, Yonsei University,
134 Shincho-dong, Seodaemun-gu, Seoul 120-749, Korea
(*Received 12 June 2003 • accepted 1 December 2003*)

Abstract−Nanoporous silica membrane without any pinholes and cracks was synthesized by organic templating method. The tetrapropylammoniumbromide (TPABr)-templating silica sols were coated on tubular alumina composite support (γ-Al_2O_3/α-Al_2O_3 composite) by dip coating and then heat-treated at 550 °C. By using the prepared TPABr templating silica/alumina composite membrane, adsorption and membrane transport experiments were performed on the CO_2/N_2, CO_2/H_2 and CH_4/H_2 systems. Adsorption and permeation by using single gas and binary mixtures were measured in order to examine the transport mechanism in the membrane. In the single gas systems, adsorption characteristics on the α-Al_2O_3 support and nanoporous unsupport (TPABr templating SiO_2/γ-Al_2O_3 composite layer without α-Al_2O_3 support) were investigated at 20-40 °C conditions and 0.0-1.0 atm pressure range. The experimental adsorption equilibrium was well fitted with Langmuir or/and Langmuir-Freundlich isotherm models. The α-Al_2O_3 support had a little adsorption capacity compared to the unsupport which had relatively larger adsorption capacity for CO_2 and CH_4. While the adsorption rates in the unsupport showed in the order of $H_2>CO_2>N_2>CH_4$ at low pressure range, the permeate flux in the membrane was in the order of $H_2 \gg N_2>CH_4>CO_2$. Separation properties of the unsupport could be confirmed by the separation experiments of adsorbable/non-adsorbable mixed gases, such as CO_2/H_2 and CH_4/H_2 systems. Although light and non-adsorbable molecules, such as H_2, showed the highest permeation in the single gas permeate experiments, heavier and strongly adsorbable molecules, such as CO_2 and CH_4, showed a higher separation factor (CO_2/H_2=5-7, CH_4/H_2=4-9). These results might be caused by the surface diffusion or/and blocking effects of adsorbed molecules in the unsupport. And these results could be explained by surface diffusion.

Key words: Surface Diffusion, Knudsen Diffusion, Blocking Effect, Silica Membrane, Adsorption, TPABr, Templating Method, Separation Factor

INTRODUCTION

The importance of membranes for gas separation has been increasingly recognized in many applied fields. Because membrane systems as gas separation apparatus will be more or less competitive at small and intermediate scale level in which flexibility of operation is desired, they may eventually challenge the present commercial status of cryogenics and pressure swing adsorption (PSA). Furthermore, microporous inorganic membranes have attracted considerable attention for gas separation due to their excellent thermal and chemical stability, good erosion resistance and high-pressure stability compared to conventional polymeric membranes. Many efforts have been made to overcome the disadvantages in inorganic membranes, which stemmed from poor membrane performance such as low selectivity and low permeability. Especially, new inorganic materials have been developed to improve selectivity and permeability [Bhave, 1991; Raman and Brinker, 1995; Burggraaf and Col, 1996; Yang et al., 2000; Hasegawa et al., 2002].

The transport of gases in inorganic membranes can be conducted through various mechanisms: Knudsen diffusion, viscous diffusion and surface diffusion. Also, the selective adsorption and surface diffusion of more strongly adsorbed components can contribute to the separation of gas mixture in the membrane. Four different mechanisms for separation of a gas mixture through a porous membrane can be identified: (a) Separation based on the differences in the molecular weights of the components due to Knudsen diffusion through the pores. (b) Separation based on molecular sieving caused by passage of a gas mixture through the pores while the larger molecules are obstructed. (c) Partial condensation of some components in the pores with exclusion of others and subsequent transport of the condensed molecules across the pore. (d) Selective adsorption of the more strongly adsorbed component onto the pore surface followed by surface diffusion of the adsorbed molecules across the pores [Burggraaf and Col, 1996; Rao and Sircar, 1993].

The rate of surface diffusion is determined by the surface diffusion coefficient and the adsorption equilibrium. Both factors are related to the interaction between the adsorbate and the pore surface. At very low surface concentration where each molecule diffuses independently, components are separated mainly due to the difference in the adsorbate and surface interactions. At higher surface concentration, interaction among adsorbates, in addition to the adsorbate-surface interaction, presumably affects the surface diffusion rate and the separation efficiency. Only a few studies [Lee and Oyama, 2002; West et al., 2002] on the surface diffusion of mixtures exist in the literature despite the importance of surface diffu-

†To whom correspondence should be addressed.
E-mail: leech@yonsei.ac.kr
**Present address: Department of Chemical Engineering, University College London, UK
‡This paper is dedicated to Professor Hyun-Ku Rhee on the occasion of his retirement from Seoul National University.

sion in actual separation processes. Furthermore, there is no available information on the role of the interaction among the adsorbates in surface diffusion [Hwang and Kammermeyer, 1975; Burggraaf and Col, 1996; Bae and Do, 2003].

Recently, organic templating derived amorphous/nanoporous silica membranes with uniform pore sizes and defect-free comparable to those in zeolites and polymeric types have been focused on [Keizer et al., 1988; Jia et al., 1994; Kim and Sea, 2001; Xomeritakis et al., 2003]. The main objective of this study is to determine the transport characteristics of nanoporous organic templating membrane. In this study, the nanoporous/amorphous silica composite membrane made by the silica sols templated with noncovalently bonded TPABr (tetrapropylammoniumbromide) was used [Raman and Brinker, 1995; Kim et al., 2001; Yang et al., 2002; Xomeritakis et al., 2003]. In order to understand permeation/separation characteristics of this membrane, single gas and binary mixtures such as CO_2/N_2, CO_2/H_2 and CH_4/H_2 systems (50 : 50 volume%) were applied for the experiments. Since the top layer in the membrane showed strong adsorption affinity for the molecules, adsorption and permeation experiments were executed at lower temperature ranges in order to focus on surface diffusion as the main permeation/separation mechanism. In addition, a mathematical model to predict the transport mechanism of the permeating components was applied to the experimental data. And the permeability and separation factors were presented over various operating conditions.

THEORY

In meso-porous membranes, such as /α-Al_2O_3 support, combined Knudsen and viscous flow takes place. For homogeneous media and/or pure non-adsorbable gases, the total permeability can be expressed by

$$F_0 = F_{0k} + F'_{0p}\bar{P} \tag{1}$$

Where F_{0k} is the permeability by Knudsen diffusion and $F'_{0p}\bar{P}$ the contribution by viscous flow which is linearly dependent on the mean pressure $\bar{P}$ in the system and transport data of membranes can be expressed in terms of flux (mol/m^{2}sec) or as flux normalized per unit of pressure (in mol/m^{2}secPa)

$$F_{0k} = \frac{2\varepsilon\mu_k\bar{r}\bar{v}}{3RTL} \tag{2}$$

$$F'_{0p} = \frac{\varepsilon\mu_p\bar{r}^2}{8\eta RTL} \tag{3}$$

where ε is the porosity, $\bar{r}$ the model pore radius of the medium, μ_k and μ_p shape factors which are assumed to be equal to the reciprocal tortuosity of the medium, R the gas constant, T the temperature, $\bar{P}$ the mean pressure, η the viscosity of the gas and $\bar{v}$ the average molecular velocity.

$$\bar{v} = \left(\frac{8RT}{\pi M}\right)^{1/2} \tag{4}$$

where M is the molecular weight of the molecules.

The relative contribution of laminar flow to the total flow is determined by the ratio of the mean free path of the gas molecules to the modal pore size. At low pressures and high temperatures, Knudsen diffusion is the predominant transport mechanism in small pores.

Since molecules adsorbed on solid surfaces may have considerable mobility, additional gas transport exists as a surface flow in the direction of decreasing surface flow, and it is detected as a deviation of the total permeability from the gas phase permeability, given by Eqs. (1)-(3). The gas phase permeability for adsorbable gases can be calculated from permeability data for non-sorbable gases with Eqs. (2) and (4). In the case of low surface concentrations, the most general description for the surface permeability F_s (mol/m^2·sec) is the two-dimensional form of Fick's law as follows:

$$F_s = -\rho(1-\varepsilon)\frac{D_s}{k_s^2}\cdot\frac{dq}{dl} \tag{5}$$

Where ρ is the density of the medium, D_s the surface diffusion coefficient, k_s^2 the tortuosity of the surface, dq/dl the concentration gradient of the adsorbed species adsorbed.

Assuming a linear pressure gradient, the integrating results of Eq. (5) for the surface permeability is

$$F_{0s} = \frac{F_s}{\Delta P} = \frac{\rho(1-\varepsilon)D_s}{k_s^2 L}\cdot\frac{dq}{dp} \tag{6}$$

Where ΔP is the pressure difference and L is the thickness of the porous medium. The term dq/dP is given by the adsorption isotherm. The surface diffusion coefficient can be calculated from Eq. (6) if the other parameters are known.

$$\rho(1-\varepsilon)q = \frac{S_v}{A_0 N_{av}}x_s \tag{7}$$

where S_v is the surface area, A_0 is the surface of an adsorbed molecule, N_{av} is Avogadro's number and x_s is the percentage of occupied surface compared to a monolayer.

$$S_v = \frac{2\varepsilon}{\bar{r}} \tag{8}$$

From Eqs. (6) to (8)

$$F_{0s} = \frac{F_s}{\Delta P} = \frac{2\varepsilon\mu_s D_s}{\bar{r}LA_0N_{av}}\cdot\frac{dx_s}{dP} \quad (\mu_s = 1/k_s^2) \tag{9}$$

Eqs. (1) and (9) can be added for a more complete picture of flow through porous media. If the mean pore radius of the porous separation layer is taken as the variable, the total equation will be

$$F_0 = F_{0k} + F_{0v}\bar{P} + F_{0s} \tag{10}$$

For a multi-layer system, the total permeability, F_0, can be expressed by using a series model.

$$F_0 = \left(\sum_i \frac{1}{F_{0,i}}\right)^{-1} \tag{11}$$

Where $F_{0,i}$ is the permeability of layer i given by Eq. (1) and takes into account the surface permeability (Eq. (6) or (9)). In a two-layer system consisting of a top (separation) layer on a porous support, the permeability data can be corrected for the support by using Eq. (11) if F_{0k} and F'_{0p} of the support are known. Knudsen flow is inversely proportional to the square root of the molecular weight.

$$\alpha_{ideal} = \sqrt{\frac{M_x}{M_y}} \tag{12}$$

where y is the mole fraction of the faster permeating component in

the permeate, and x the mole fraction of this component in the feed [Keizer et al., 1988; Uchytil, 1994; Burggraaf and Col, 1996]. In this regime, light gases permeate more rapidly than heavy ones. The ideal Knudsen separation factor for binary mixture equals the square root of the ratio of molecular masses. The presence of surface diffusion influences the ideal separation factor α. The actual separation factor, α, is defined as [Burggraaf and Col, 1996]

$$\alpha_{actual} = \frac{y}{1-y} \cdot \frac{1-x}{x} \quad (13)$$

PREPARATION OF MEMBRANE

1. Preparation of TPABr-Templating Silica Sols

The organic templating silica sols were prepared by mixing silica sols with organic template (TPABr, 3-9 wt%) at room temperature and then aged at 50 °C for 12 h. Silica sols were prepared from tetraethoxysilane (TEOS) by using a two-step acid catalyzed procedure [Yang et al., 2002]. A final molar ratio of the silica sol was TEOS : EtOH : H_2O : HCl of 1.0 : 3.8 : 5.0 : 0.0053. The silica-template hybrid composite was prepared by evaporating organic templating silica sols in polystyrene dishes, and the unsupported membrane was prepared by heating silica gels at 600 °C (heating rate, 1 °C/min, holding time 2 h).

2. Preparation of TPABr-Templating Silica Membrane

The porous support tubes(8mm outside diameter, 0.8 mm thickness, 100 mm length, and 0.1 μm mean pore diameter) were fabricated by the usual slip-casting procedure using a slurry of /α-Al_2O_3 powder (AES-11, Sumitomo Co.). γ-Al_2O_3/α-Al_2O_3 composite supports were prepared by a dip-coating of boehmite sols on tubular α-Al_2O_3 supports. The average pore size of the γ-Al_2O_3 layer was 2.8 nm measured by SEM. The details for the these supports were given in previous work [Yang et al., 2002]. The organic template-derived silica composite membranes were prepared by a dip-coating of the templating sols on the γ-Al_2O_3/α-Al_2O_3 composite supports at room temperature followed by heating to 550 °C at a heating rate of 1 °C/min, holding for 2 h. And the nanoporous/amorphous silica composite membrane was synthesized by sol-gel process using silica sols templated with noncovalently bonded TPABr. In this study, the support symbolizes tubular α-Al_2O_3 support and the unsupported symbolizes TPABr templating silica/γ-Al_2O_3 layer.

EXPERMENTAL

1. Adsorption Behavior Measurement

The schematic apparatus of the adsorption experiment is shown in Fig. 1. The kinetics and equilibrium of adsorption were measured by the gravimetric method using an electrobalance (model Cahn 2000, Houston Ins., USA). About 200 mg of the prepared the unsupport and the support were put into the basket in the hangdown tube of the electrobalance. The basket was made of aluminum mesh to make it easy to emit the heat of adsorption into the gas phase. The unsupport in the basket was regenerated for 12 hours at 200 °C in vacuum condition. The system was evacuated to the extent of less than 10^{-4} mmHg by the vacuum pump before the experiment. A mercury manometer was used to measure the pressure of the gas in the system. A circulating thermostat (Model Rec-11, Jeiotech Co., Korea) was used to keep the temperature of the system constant.

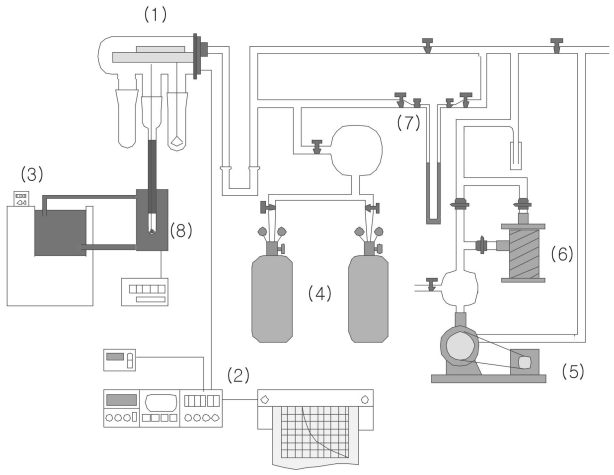

Fig. 1. Schematic diagram of gravimetric apparatus for adsorption measurements.

1. Electric cahn balance 2000
2. Integrator
3. Chiller
4. Gas bomb
5. Vacuum pump
6. Moisture trap
7. Mercury manometer
8. Adsorber basket

The feed gas was supplied to the system by the gas regulator and fine valve within a short period of time. The pressure of the feed gas was increased in a stepwise procedure from 0 atm to 0.8 atm and the uptake curve was measured at each pressure range. The step increase of the pressure in the system was sustained within the range of 30-80 mmHg. In order to prevent the system from being contaminated by the pollutant, the system was rinsed with He for more

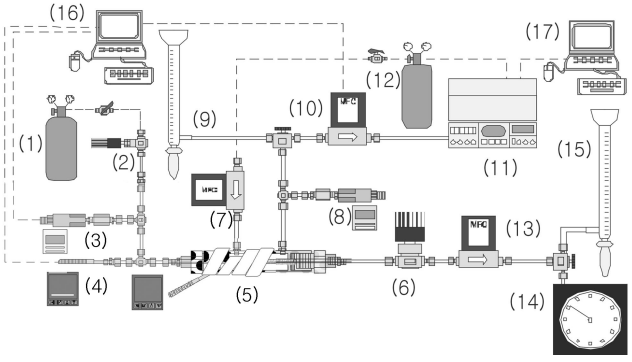

Fig. 2. Schematic diagram for gas permeation and separation measurements.

1. Feed gas
2. Metering valve
3. Feed pressure transducer
4. RTD & temperature controller
5. Membrane cell
6. Back pressure regulator
7. MFC (sweep gas control)
8. Permeate pressure transducer
9. Soap bubble flow meter (permeate)
10. MFM (permeate flow)
11. GC (TCD)
12. GC carrier & sweeping gas (He)
13. MFC (stage cut control)
14. Wet gas flow meter (retentate)
15. Soap bubble flow meter (retentate)
16, 17. Data interfacing computer

than 2 hours after finishing each experiment. From these data, the adsorption amount and diffusional time constant of each molecule in the support and the unsupport could be obtained [Ahn et al., 2002].

2. Membrane Transport Measurement

The schematic apparatus of the transport of membrane, the support and the unsupport, experiment is shown in Fig. 2. In the tubular type membrane, its inner diameter was above 6.2 mm and full length was about 86.0 mm. The effective area of this membrane for permeation was 15.19 cm^2. The membrane was placed in the stainless module that is tubular type Wicke-Kallenbach membrane cells with body, disks and rids. Silicon O-rings were used as seals between the membrane and the module. In order to prevent separated/permeated gas from stagnating in the cell, the cell consisted of sweeping gas inlet line and 3-way outlet line.

Thermocouples (RTD type/Pt 100 Ω) were equipped at the inlet gas line, inner cell and outer cell to measure the system temperature. In particular, in the case of the inner cell temperature, a thermocouple was placed into the center of the cell by pass-through type. A heating block was set up on the cell and pre-heater (electrical heating tape) was wrapped in front of inlet gas line. These two heaters were controlled by two temperature controllers (Eurotherm Co., USA). Pressures were measured by the two pressure transducers (Sensyst Co., USA) located at inlet and permeate of membrane cell that were calibrated by pressure gauge (HEISE Co., USA). Feed gas was controlled by MFC (Mass Flow Controller, Tylan Co., USA) and pressure regulator (Harris Co., USA) of gas cylinder, and retentate gas was controlled by another MFC and back-pressure regulator. The flow rates of retentate and permeated gases were measured by soap bubble flow meter (Supelco Co., USA), MFC and wet gas meter (Sinagawa Co., Japan) according to each condition.

In the case of mixed gases, the composition of separated gas ingredients was analyzed by online Gas Chromatography (model 5890 II, Hewlett Packard, TCD type, USA) with auto injection 6-way valve system (Valco. Co., USA). And helium was used as the carrier and sweeping gas. In order to prevent the system from being contaminated by the other gases, the feed and permeate sides of the membrane were swept with the helium gas for more than 10 minutes and the system was heat-treated (>100 °C) before beginning each experiment.

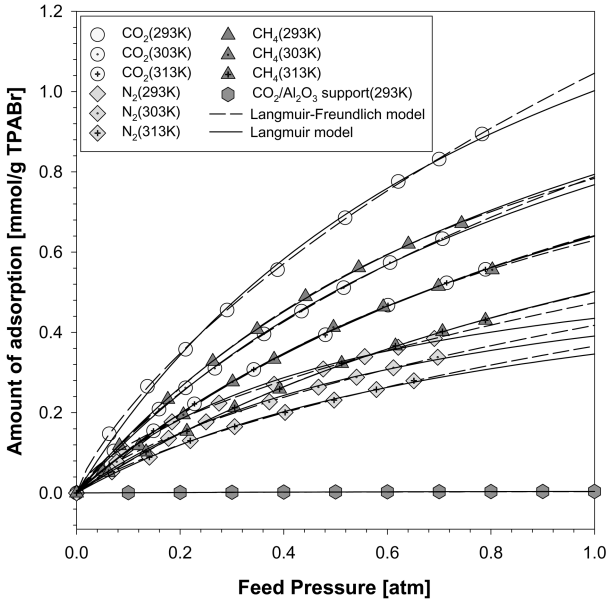

Fig. 3. Equilibrium isotherm curves of CO_2, N_2 and CH_4 on TPABr templating SiO_2/γ-Al_2O_3 composite layer and α-Al_2O_3 at 293.15-313.15 K and 0-1 atm.

Single gas permeation was measured by dead-end mode with

Table 1. Equilibrium adsorption parameters of TPABr templating silica layer applied to Langmuir and Langmuir-Freundlich model

Temp. [K]	Model		(a) CO_2			(b) N_2			(c) CH_4		
			Q_m	b	n	Q_m	B	N	Q_m	b	n
Support (α-alumina support)											
293.15 K	Langmuir	Value	0.0090	0.7730							
		err (%)	0.0003	0.0411							
	L/F	Value	0.0093	0.7194	1.0175						
		err (%)	0.0013	0.1704	0.0557						
Unsupport (TPABr templating silica/γ-alumina composite layer)											
293.15	Langmuir	Value	1.9260	1.0847	-	0.6631	1.9084	-	1.6046	0.9787	-
		err (%)	0.0970	0.0873	-	0.0360	0.1974	-	0.0333	0.0307	-
	L/F	Value	4.8055	0.2782	1.2658	3.0025	0.1873	1.5254	1.4075	1.2562	0.9430
		err (%)	0.9034	0.0653	0.0322	1.1699	0.0865	0.0574	0.0588	0.1044	0.0186
303.15	Langmuir	Value	1.6191	0.9024	-	0.6585	1.4627	-	1.5003	0.7463	-
		err (%)	0.0463	0.0372	-	0.0345	0.1312	-	0.0636	0.0451	-
	L/F	Value	2.2621	0.5341	1.1002	1.7539	0.3125	1.3340	1.1788	1.1471	0.9087
		err (%)	0.2067	0.0701	0.0223	0.4102	0.0931	0.0456	0.0813	0.1527	0.0281
313.15	Langmuir	Value	1.4523	0.7869	-	0.6566	1.1142	-	1.2501	0.6702	-
		err (%)	0.0263	0.0208	-	0.0324	0.0838	-	0.0306	0.0228	-
	L/F	Value	1.6304	0.6529	1.0371	1.3405	0.3754	1.2011	1.1718	0.7433	0.9802
		err (%)	0.1095	0.0680	0.0195	0.3110	0.1137	0.0433	0.0970	0.0994	0.0251

the retentate stream blocked while mixed gas permeation was measured by through-flow type in order to control stage-cut. Single/Mixed gas permeation was measured under temperature ranges of 293-373 K and pressure ranges of 0-5 atm range for H_2, N_2, CO_2, CH_4, and their mixtures such as CO_2/N_2, CH_4/H_2 and CO_2/N_2.

RESULTS AND DISCUSSION

1. Adsorption Characteristics of α-Al_2O_3 Support

In this study, the adsorption characteristics of the α-Al_2O_3 support (support) and TPABr templating silica/γ-Al_2O_3 composite layer (unsupport) were measured to investigate the transport mechanism on both parts instead of TPABr templating silica/γ-Al_2O_3/α-Al_2O_3 composite membrane.

Adsorption isotherms of CO_2, N_2 and CH_4 on the unsupport and CO_2 on the support are presented in Fig. 3. The experimental adsorption data were well fitted to the Langmuir isotherm model (Eq. (14)) and Langmuir-Freundlich isotherm model (Eq. (15)). The isotherm parameters of theses models are presented in Table 1.

$$\text{Langmuir isotherm:} \quad q = q_o \cdot \frac{bP}{bP+1} \tag{14}$$

$$\text{L-F isotherm:} \quad q = q_o \cdot \frac{bP^{1/n}}{bP^{1/n}+1} \tag{15}$$

Adsorption experiments of the support were executed to confirm the existence of surface diffusion on it. In the CO_2/support system, the adsorption isotherm was almost linear with pressure. In addition, the amount of CO_2 adsorption on the support could be negligible compared to the unsupport.

Surface diffusion is known as one of the important transfer mechanisms in nanoporous adsorbents [Lee and Oyama, 2002; Kapoor et al., 1989; Bhandarkar et al., 1992]. However, owing to larger pores (about 100 nm) and lower chemical affinity, the support had weak

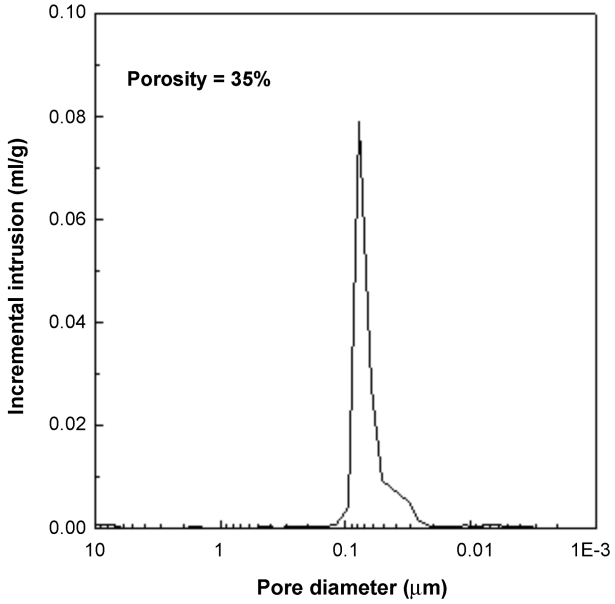

Fig. 4. Pore size distribution of α-Al_2O_3 support measured by mercury porosimetry.

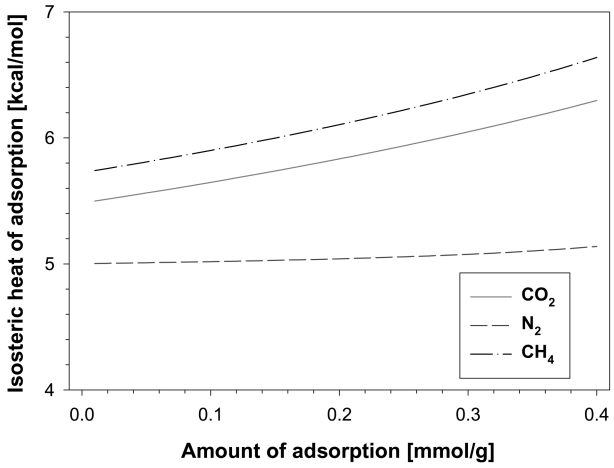

Fig. 5. Isosteric heat of adsorption of CO_2, N_2 and CH_4 on TPABr templating SiO_2/γ-Al_2O_3 composite layer.

adsorption capacity compared to the unsupport as shown in Fig. 3. This result implied that surface diffusion caused by adsorption could be neglected in case of support.

The textural properties of the support were analyzed by mercury porosimetry in Fig. 4. The average pore diameter of the support was about 100 nm, and it showed a narrow and steep single pore size distribution curve. In the case of this pore structure, the diffusion mechanism of the support may be dominated by viscous diffusion (or Poiseuille diffusion) or Knudsen diffusion. Especially Knudsen number, Kn (Eq. (16)), defined by the ratio between mean free path (λ) (Eq. (17)) and average pore diameter (d_p) is lower than 1.0 (Fig. 5).

$$\text{Knudsen number:} \quad Kn = \frac{\lambda}{d_p} \tag{16}$$

$$\text{Mean free path:} \quad \lambda = \frac{3.2\mu}{P}\left(\frac{RT}{2\pi M}\right)^{1/2} \tag{17}$$

It signifies that the diffusion mechanism of the α-Al_2O_3 support is more influenced by viscous diffusion than Knudsen diffusion. Moreover, it is very hard for surface diffusion to contribute to the diffusion on the α-Al_2O_3 support. It was also confirmed that effective separation on the α-Al_2O_3 support could not be expected by difference between pore and molecular size.

2. Adsorption Characteristics of TPABr Templating Silica/γ-Al_2O_3 Layer

Separation ability in organic templating silica/alumina composite membrane would be determined by properties of unsupport (TPABr templating silica/γ-Al_2O_3 composite top layer) rather than α-Al_2O_3 support even though thickness of the unsupport is much smaller than the support. The adsorption experiments for single component were studied on the unsupport in order to elucidate the effect of surface diffusion on the transport mechanism.

The isotherm curves of each molecule on the unsupport were non-linearly proportional to feed pressure and showed Type I following the BDDT classification [Bond, 1967]. The Langmuir-Freundlich model (an average error of approximation ε=0.209%) predicted data with higher accuracy than the Langmuir model (ε=0.491%)

Table 2. A comparison of structural, physical, and electronic parameters for the gases in the present work

	CO_2	N_2	CH_4	H_2
Kinetic diameter [Å]	4.00	3.68	3.82	2.92
Interaction	Lateral (strong)	Vertical	Lateral (strong)	-
Structure	Linear	Linear	Tetrahedral	Linear
Polarizability α [10^{-40} $J^{-1}C^2m^2$]	2.93	1.97	2.89	0.911

in Fig. 3.

As shown in Fig. 3, the adsorption amount on the unsupport was of the order of CO_2>CH_4>N_2. And the adsorption amounts CH_4 and CO_2 on the unsupport were much higher than that of N_2 due to interaction and polarity of each adsorbate, as can be seen in Table 2. Since the amount of equilibrium adsorption of CO_2/unsupport system was approximately 1/3rd of the CO_2/Zeolite 4A system [Ahn et al., 2002], the adsorption capacity of the unsupport might affect the permeate mechanism of silica/alumina composite membrane.

The effect of temperature on the adsorption of CO_2 and CH_4 was larger than that on the adsorption of N_2. Moreover, as shown in Fig. 5, the isosteric heats of adsorption ($-\Delta H_s$) of molecules (CO_2, N_2, CH_4) from Clausius-Clapeyron Eq. (18) were below 7 Kcal/mol. This result implied physisorption by Van der Waals force or Coulomb force on the surface of the unsupport [Yang, 1987].

$$\text{Clausius-Clapeyron equation:} \quad -\Delta H_s = RT^2\left(\frac{\partial \ln P}{\partial T}\right)_n \tag{18}$$

Ross et al. [1964] and Talu et al. [1987] showed that the relation between coverage and isosteric heat of adsorption explains the interaction characteristics in the heterogeneous surface. For heterogeneous surfaces in the micro/nanopores of some adsorbents, the vertical interactions between the solid surface molecules and gas molecules decrease as coverage increases, while the lateral interactions between the adsorbed molecules increase with coverage. As can be seen in Fig. 5, CO_2 and CH_4 showed an increase in $-\Delta H_s$ with an increase in the coverage. It signifies that lateral interaction between adsorbates caused by Van der Waals force is dominant [Yang, 1987].

The parameter, $n \approx 1$, the so-called mono layer adsorption, in the L-F model for CO_2 and CH_4 represents that each molecule is occupying just one site. Moreover, since CO_2 and CH_4 have a relatively high value of polarity in Table 2, a columbic (electrostatic) force may be generated between each adsorbed molecule. These results suggested strongly that the surface diffusion originated by hopping between previously adsorbed molecules can be occurring on the unsupport [Talu and Kabe, 1987].

On the other hand, N_2 showed almost constant in $-\Delta H_s$ with an increase in the coverage as shown in Fig. 5. It implies that lateral interaction was offset by vertical interaction [Yang, 1987]. Because the polarity of N_2 molecules is relatively lower than that of CO_2 or CH_4, the affinity and amount of adsorption of N_2 are also lower than them. Besides the parameter, $n \approx 1.35$ (average value) in the L-F model (Eq. (15)) in N_2 represents that each molecule is occupying one or more sites. Therefore, in the case of weakly adsorbable gases such as N_2 or H_2, it is not necessary to consider hopping phenomena and surface diffusion between adsorbed molecules in the pores of the unsupport.

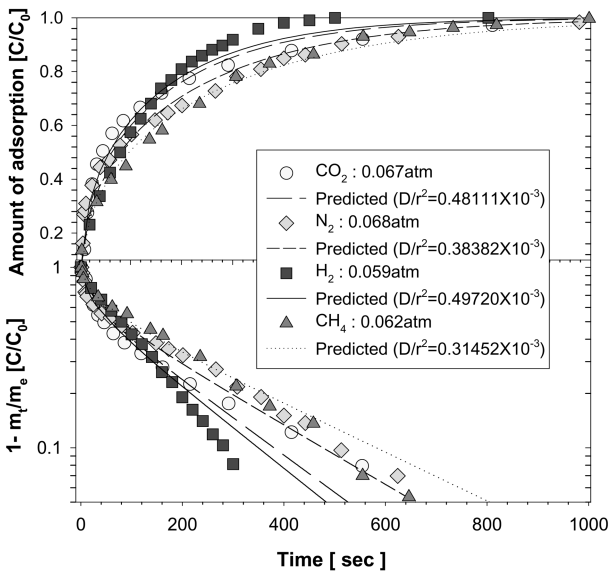

Fig. 6. Experimental adsorption uptake curves of CO_2, N_2, CH_4 and H_2 with predicted results by isothermal model on TPABr templating SiO_2/γ-Al_2O_3 composite layer at 293 K.

In Fig. 6, diffusional time constants in the unsupport were calculated by the experimental uptake curve for each molecule at every step of pressure variation. Adsorption rates showed in the order of H_2>CO_2>N_2>CH_4. Diffusional time constants in low pressure range were obtained from the experimental uptake curve by using Fick's law (Eq. (19)) and its numerical solution (Eq. (20)) [Karger and Ruthven, 1992].

$$\text{Fick's second law:} \quad \frac{\partial q}{\partial t} = \frac{1}{r^2}\cdot\frac{\partial}{\partial r}\left(r^2\cdot D_e\cdot\frac{\partial q}{\partial r}\right) \tag{19}$$

$$\text{Numerical Solution:} \quad \frac{m_t}{m_e} = 1 - \frac{6}{\pi^2}\sum_{n=1}^{\infty}\frac{1}{n^2}\exp\left(\frac{-n^2\pi^2 D_e t}{r^2}\right) \tag{20}$$

The obtained diffusional time constants, D_e/r^2, were in order of H_2>CO_2>N_2>CH_4 as shown in Fig. 6. The value of D_e/r^2 in H_2/unsupport system is higher than any other gases. Because it is nonpolar (polarizability=0.911), lightest molecular weight (2.0 mol/g), smallest kinetic diameter (2.92 Å) and linear structure, it can diffuse pore walls very quickly and is not disturbed by any hindrance. The strongest adsorbate, CO_2, in this study has high value in D_e/r^2 in spite of its large kinetic diameter (4.00 Å). It stemmed from the strong adsorption affinity of CO_2 on the unsupport in Fig. 3. However, the diffusion rate of CH_4 with smaller kinetic diameter (3.82 Å) than CO_2 showed slower than those of other gases in the unsupport pore in Fig. 6 although CH_4 also showed relatively large adsorption amount in Fig. 3. It implies that there is a molecular structural effect on the pore diffusion in the unsupport. The diffusion of CH_4 molecules in the pore of the unsupport might be interrupted by steric hindrances because of its tetrahedral structure (Table 2), which is different from CO_2 molecules with linear structure.

3. Permeate Properties of Alumina Membrane Support

A permeate experiment of α-Al_2O_3 support was performed with CO_2, N_2, CH_4 and H_2 at 293-373 K temperature and 0-5 atm pres-

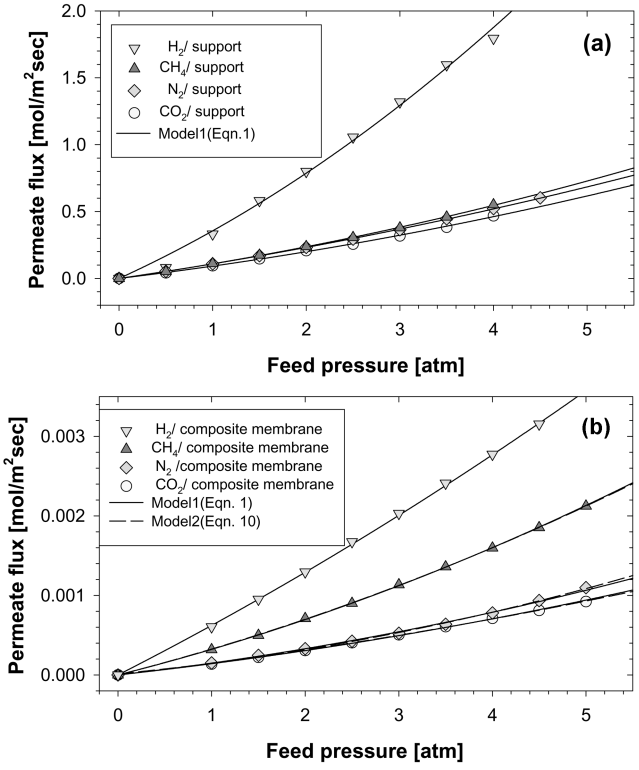

Fig. 7. Permeate fluxes of CO_2, N_2, CH_4 and H_2 on (a) α-Al_2O_3 support and (b) TPABr templating silica/alumina composite membrane at 293 K with predicted curves by the permeation method model (Eq. (1)) and surface diffusion model (Eq. (10)).

sure range. Fig. 7(a) shows the permeate molar flux of H_2, N_2, CH_4 and CO_2 at α-Al_2O_3 support as a function of pressure. The permeate flux in the support was inversely proportional to molecular weight ($H_2 \gg N_2 > CH_4 > CO_2$). Namely, the light molecules, such as H_2, showed much higher permeate flux than the heavy molecules, such as CO_2, CH_4 and N_2. As mentioned above, Knudsen number (Eq. (16)) of each molecule was lower than 1.0, because the average pore diameter (Fig. 4) was too large between molecules for collisions. It

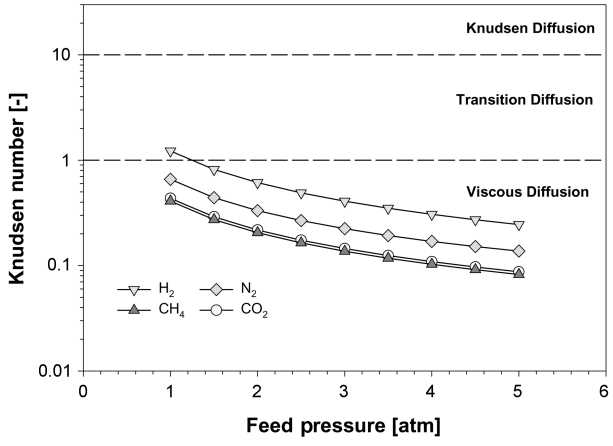

Fig. 8. Knudsen numbers of CO_2, N_2, CH_4 and H_2 on α-Al_2O_3 support at 293 K (Eq. (16)).

Table 3. Pure gas permeabilities due to the Knudsen-viscous Poiseuille diffusion on α-Al_2O_3 support at 293 K and 313 K

	293 K		313 K	
	F_{0p}	F_{0k}	F_{0p}	F_{0k}
CO_2	0.230841	0.058569	0.153448	0.068831
N_2	0.124997	0.110387	0.178797	0.082174
H_2	0.786066	0.257588	0.745229	0.242525
CH_4	0.138633	0.093005	0.137412	0.088103

signifies that the permeate mechanism of support depends on viscous diffusion mainly as shown in Fig. 8. Therefore, the permeate model (Eq. (1)) could be applied for examining transport mechanism of α-Al_2O_3 support since the model is combined with viscous and Knudsen diffusions. And the each permeability can be calculated by fitting experimental data. Using these method, the effective mean pore size and geometric factors of inorganic membrane can be calculated (Eq. (20)).

As mentioned above, the Knudsen diffusion permeability (F_{0k}) was negligibly smaller than viscous diffusion permeability (F'_{0p}) in the α-Al_2O_3 support [Keizer et al., 1988; Uchytil, 1994; Burggraaf and Col, 1996]. As a result, the effective mean pore radius of α-Al_2O_3 support calculated by Eq. (20) was about 118.7 nm (average value).

$$\bar{r} = \frac{16\eta\mu_k\bar{v}}{3\mu_p} \cdot \frac{F_{0k}}{F'_{0p}} \tag{20}$$

This value was in a good agreement with the actual value (100 nm) obtained from porosimetry in Fig. 3 and Table 3 [Yang et al., 2002; Uchytil, 1994]. It also proved that the permeate mechanisms of α-Al_2O_3 support follows viscous diffusion.

4. Permeation and Separation Properties of TPABr Templating Silica Membrane

Uniform dispersion of the TPABr template in the silica matrix was confirmed by NMR spectroscopy. And TPA template-derived silica composite membrane (TPABr templating silica/alumina composite membrane) without any defect could be prepared by dip coating the silica sol. The average pore size and specific surface area of the unsupported membrane were below 18 Å and about 830 m^2/g, respectively [Yang et al., 2002]. Fig. 7(b) shows the permeate flux of pure gases such as H_2, N_2, CH_4 and CO_2 on the composite membrane at 293 K as a function of pressure. The permeate molar fluxes of H_2, N_2, CH_4 and CO_2 were 0-0.005 mol/m^2sec and the amount of permeate fluxes of these molecules was in the order of $H_2 > CH_4 > N_2 > CO_2$.

Table 4. Pure gas permeabilities due to the Knudsen-viscous Poiseuille diffusion on TPABr templating composite layer at 293 K and 313 K

	293 K		313 K	
	F_{0p}	F_{0k}	F_{0p}	F_{0k}
CO_2	2.3143×10^{-8}	1.0611×10^{-7}	8.1481×10^{-8}	8.2032×10^{-8}
N_2	3.1510×10^{-8}	1.0109×10^{-7}	1.5349×10^{-7}	1.4513×10^{-7}
H_2	4.5765×10^{-8}	5.5275×10^{-8}	7.7718×10^{-9}	4.5541×10^{-7}
CH_4	5.1536×10^{-8}	2.4349×10^{-7}	4.4991×10^{-8}	2.3745×10^{-7}

Table 5. Pure gas permeabilities due to the surface diffusion on TPABr templating composite layer at 293 K and 313 K

	293 K			313 K		
	F_{0p}	F_{0k}	F_{0s}	F_{0p}	F_{0k}	F_{0s}
CO_2	5.7178×10^{-18}	9.8866×10^{-7}	1.1695×10^{-9}	1.6248×10^{-17}	2.7004×10^{-5}	3.9652×10^{-6}
N_2	2.1641×10^{-2}	2.1038×10^{-5}	6.3599×10^{-5}	2.4645×10^{-3}	8.6799×10^{-6}	1.3709×10^{-4}
CH_4	9.6892×10^{-18}	2.4952×10^{-5}	2.5121×10^{-8}	2.4246×10^{-3}	2.3536×10^{-5}	2.3206×10^{-4}

In Fig. 7(b), the permeate flux of H_2 with lower adsorption affinity and smallest kinetic diameter is linearly proportional to its feed pressure. It indicates that the permeate mechanism in H_2/composite membrane system follows Knudsen diffusion. Also in the case of N_2, the permeate flux in Fig. 7(b) was well fitted by the permeate method model (Eq. (1)) because it had low adsorption capacity and diffusivity on the TPABr templating silica membrane in Fig. 3. Therefore, the surface diffusion in the permeate mechanism of H_2 or N_2 was also negligible. However, in the case of CO_2 and CH_4, there were some deviations between the permeate model (Eq. (1)) and the surface diffusion model (Eq. (10)) because of their large adsorption capacity on the unsupport in Fig. 3. Tables 4 and 5 contain these permeabilities as fitting parameters. In the case of Table 4, the permeate method model (Eq. (1)) was used. On the other hand, in the case of Table 5, the surface diffusion model (Eq. (10)) was applied.

To characterize the membrane separation mechanism, especially surface diffusion, a separation experiment should be executed in the strongly adsorbable/weakly adsorbable mixture systems, for example CO_2/N_2, CO_2/H_2 and CH_4/H_2 systems.

In Fig. 9, the more permeate flux, the less separation factor with an increase of feed pressure. The permeate fluxes of CO_2/N_2 mixture were 0.0-8.0×10^{-5} mol/m^2sec at 0-5 atm pressure range. In this system, the actual separation factors were 6.0-7.0 even though the ideal Knudsen separation factor of the mixture is 0.7977. It stemmed from the effect of surface diffusion on the membrane separation.

Moreover in the case of CO_2/H_2 and CH_4/H_2 mixture systems, CO_2 and CH_4 molecules, that are heavy-weighted and strongly adsorbable, gas permeated much more than H_2 in Figs. 10 and 11. The

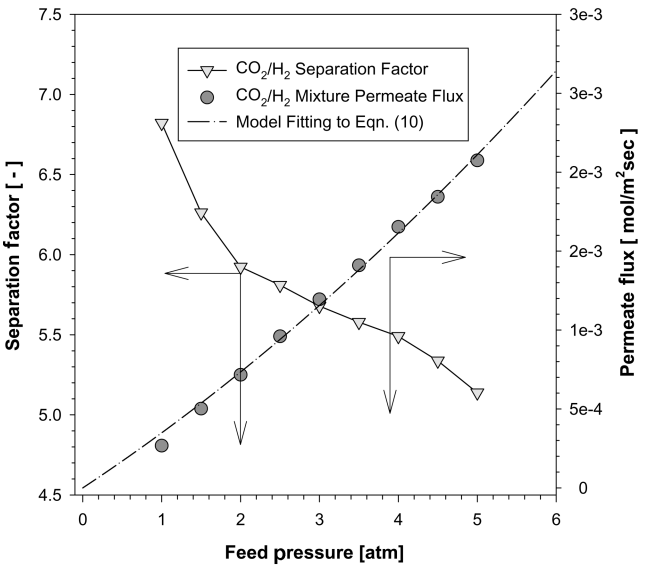

Fig. 10. Permeate flux and separation factor of CO_2/H_2 mixture on TPABr templating silica/alumina composite membrane at 313 K.

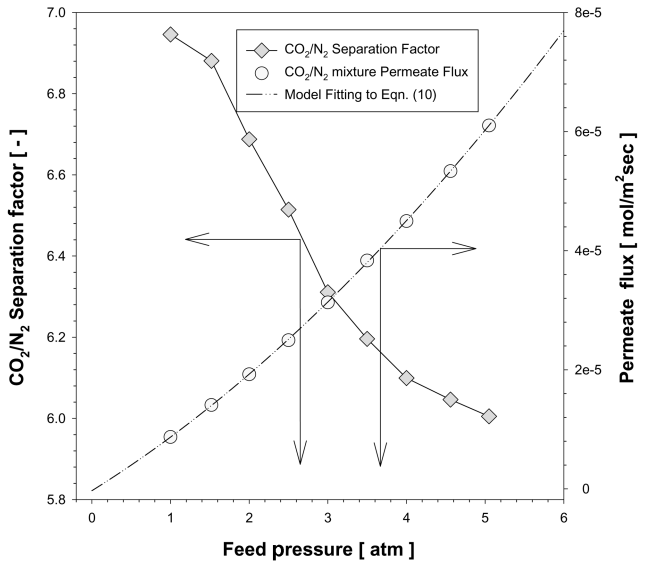

Fig. 9. Permeate flux and separation factor of CO_2/N_2 mixture on TPABr templating silica/alumina composite membrane at 313 K.

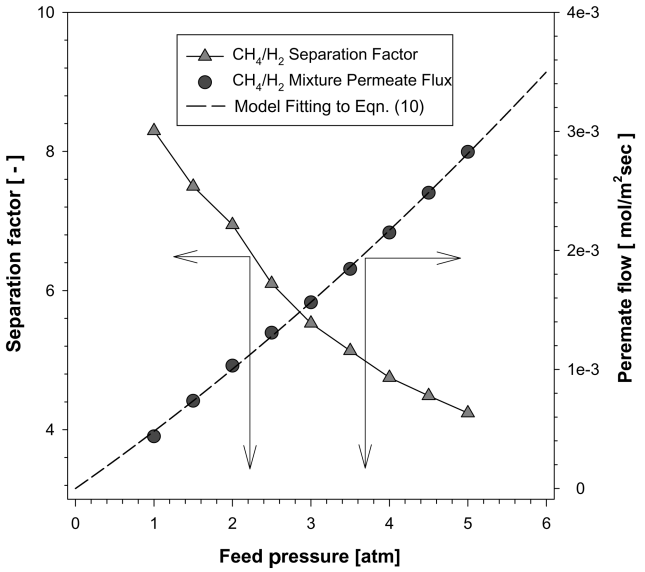

Fig. 11. Permeate flux and separation factor of CH_4/H_2 mixture on TPABr templating silica/alumina composite membrane at 313 K.

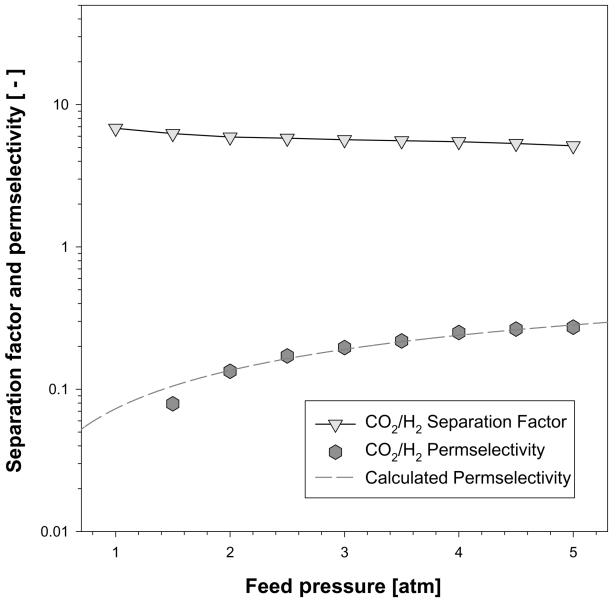

Fig. 12. Comparison between separation factor and permselectivity in CO_2/H_2 mixture at 313 K.

more CO_2/H_2 and CH_4/H_2 mixtures permeate flux, the less separation factor with an increase of feed pressure. These results indicated that strongly adsorbable molecules are more selective than weakly adsorbable molecules in this membrane. The separation factors of the CO_2/H_2 mixture were in 5.0-7.0 range and the permeate fluxes were in 0-3×10^{-3} mol/m^2sec at 0-5 atm pressure range as shown in Fig. 10. The separation factors of CH_4/H_2 mixture were in 4.0-9.0 range and the permeate fluxes were in 0-4×10^{-3} mol/m^2 sec at 0-5 atm pressure range in Fig. 11.

Fig. 12 shows a comparison between the separation factors and permselectivities in the CO_2/H_2 mixture. Where permselectivity is the permeability of flux ratio between two single gases (Eq. (21)), not mixed gases.

$$\alpha_{Perm,A/B}=\frac{F_{O.A}}{F_{O.B}} \tag{21}$$

There were large deviations between permselectivities and separation factors. In the pure gas transport experiment, the permeate molar flux of H_2 was much larger than that of other molecules as shown in Fig. 7(b). Therefore, the ideal Knudsen separation factor of the CO_2/H_2 mixture is 0.2132, and low permselectivities were obtained from the experimental range. However, in the CO_2/H_2 and CH_4/H_2 mixtures, the actual separation factors were much higher than the ideal Knudsen separation factors or permeabilities. It implies that surface diffusion of molecules plays a key role in the separation mechanism.

In the mixture of adsorbable/non-adsorbable molecules, the adsorbable one, CO_2 or CH_4, adsorbed strongly on the membrane pore surface due to its adsorption affinity. Then, the hopping of molecules between adsorption sites occurred by surface diffusion [Yang, 1987]. The vacant sites in the pores were occupied by adsorbable molecules, and surface concentration of adsorbable molecules became higher and higher. Furthermore, the multilayer adsorption of strongly adsorbable molecules blocks the diffusion of weakly adsorbable molecules, H_2, through the pores. As a result, strongly adsorbable molecules permeated through the membrane faster than non- or weakly adsorbable molecules.

In sum, it seems that the permeability of the weakly adsorbed molecule, especially H_2 molecule, is drastically reduced owing to the presence of the higher adsorbable molecules which showed relatively low permeability in the pure gas experiments. The more selectively adsorbed component, such as CO_2, permeated through the membrane with very high rate. In other words, the order of permeabilities of the molecules followed in order of their adsorption affinity on the silica unsupported membrane. And it demonstrates the "hindrance effect" or "structural effect" of each molecule, which can be a major characteristic of a nanoporous membrane relying on surface diffusion [Rao and Sircar, 1993]. Comparable features of mixture permeation through silica membranes have been reported in the other systems such as propene/ethane by Jolinde et al. [1998], n-butane/methane by Vroon et al. [1998] and ethane/methane by Jolinde et al. [2000].

CONCLUSIONS

The permeation/separation characteristics of nanoporous TPABr templating silica/alumina composite membrane were studied by using single gases and binary mixtures such as CO_2/N_2, CO_2/H_2 and CH_4/H_2 systems (50 : 50 volume%). The adsorption capacity of α-Al_2O_3 support was negligible compared to the silica unsupport. In the α-Al_2O_3 support, gas permeance generally depends on size differences between pores and molecules. The permeation model expressing the relative contributions of Knudsen diffusion and viscous flow through porous membrane could predict well the experimental data in the α-Al_2O_3 support. While the adsorption rates in the unsupport showed in the order of $H_2>CO_2>N_2>CH_4$ at low pressure range, the permeate flux in the membrane was in the order of $H_2\gg N_2>CH_4>CO_2$. Therefore, the permeate flux did not show any relationship with the adsorption rate. However, because the top layer in the membrane showed strong adsorption affinity for the molecules, the surface diffusion contributed to main permeation/separation mechanism.

Light and non-adsorbable molecules, such as H_2, showed the highest permeation in the single gas permeate experiments; however, heavier and strongly adsorbable molecules, such as CO_2 and CH_4, showed higher separation factor (CO_2/H_2=5-7, CH_4/H_2=4-9). Moreover, in the CO_2/H_2 and CH_4/H_2 mixtures, the actual separation factors were much higher than the ideal Knudsen separation factors because of the competitive adsorption and surface diffusion of molecules in the membrane pores, which play a key role in the separation mechanism. Therefore, the order of permeabilities of the molecules followed in the order of their adsorption affinity on the silica unsupported membrane. And the "hindrance effect" or "structural effect" of each molecule by adsorption affinity and surface diffusion should be considered as the main separation mechanism in a nanoporous silica membrane.

In the mixture of adsorbable/non-adsorbable molecules, the adsorbable one, such as CO_2 or CH_4, adsorbed strongly on the membrane pore surface due to its adsorption affinity. Then, the hopping of molecules between adsorption sites occurred by surface diffusion. The vacant sites in the pores were occupied by adsorbable mol-

ecules, and the surface concentration of adsorbable molecules became higher and higher. Furthermore, the previously adsorbed molecules along the pore wall blocked the second time adsorption of weakly adsorbable molecules. As a result, strongly adsorbable molecules permeated through the membrane more and faster than non-adsorbable or weakly adsorbable molecules.

In short, it seems that the permeation of a weakly adsorbed molecule, especially H_2 molecule, is drastically reduced owing to the strong adherence between the pore wall and the higher adsorbable molecule, though it showed relatively low permeability.

ACKNOWLEDGMENT

The financial support of KOSEF (Korea Science and Engineering Foundation, R01-1999-000-00198-0) is gratefully acknowledged.

NOMENCLATURE

A_0 : surface area of an adsorbed molecule [m^2]
b : Langmuir parameter [1/atm]
D_e : effective diffusion coefficient [m^2/sec]
D_s : surface diffusion coefficient [m^2/sec]
d_p : pore size [m]
E_{st} : isosteric heat of adsorption [kJ/mol]
F_0 : total permeability of gas [mol/m^2·sec·Pa]
F_{0k} : permeability due to Knudsen diffusion [mol/m^2·sec·Pa]
F_{0v} : permeability divided by pressure due to viscous flow [mol/m^2·sec·Pa]
F_{0s} : permeability due to surface diffusion [mol/m^2·sec·Pa]
F_s : surface permeability [mol/m^2·sec]
$(k_q)^2$: tortuosity factor for gas permeation [-]
L : thickness of the membrane system [m]
M : molecular mass of gas molecules [kg/mol]
m_e : mass adsorbed at time $t\rightarrow\infty$ [g]
m_t : mass adsorbed at time t [g]
n : number of sites that an adsorbate occupies [-]
N_{AV} : Avogadro's number [-]
$\overline{P}$: mean pressure [kPa]
ΔP : pressure difference across the membrane system [kPa]
P_r : pressure ratio (permeate pressure P_1 divided by feed pressure P_h) [-]
q : gas amount adsorbed [mmol/g]
q_m : gas amount adsorbed [mmol/g]
R : gas constant per mole [8.317J/mol·K]
$\bar{r}$: modal pore radius of the solid medium [m]
S_v : surface area of solid system per unit of volume [m^2/m^3]
t : time [sec]
T : absolute temperature [K]
$\bar{v}$: average molecular velocity [m/sec]
x_s : fraction of surface covered by adsorbed molecules [-]
x : mole fraction of faster permeating component in feed [-]
y : mole fraction of faster permeating component in permeate [-]
$-\Delta H_s$: isosteric heat of adsorption [cal/mmol]

Greek Letters

α : actual separation factor [-]
α^* : ideal (Knudsen) separation factor [-]
α_{perm} : permselectivity [-]
α_s : separation factor of support [-]
ε : porosity of the membrane system [-]
η : viscosity of the gas (mixture) [N/m^2-sec]
ρ : true density of the solid medium [kg/m^3]
μ_k : shape factor for Knudsen diffusion [-]
μ_v : shape factor for viscous flow [-]

REFERENCES

Ahn, H., Yoo, H.-K., Shul, Y., Hyun, S. and Lee, C.-H., "Diffusion Mechanism of N_2 and CH_4 in Pelletized Zeolite 4A, 5A and CaX," *J. Chem. Eng. of Jap.*, **35**, 334 (2002).

Bae, J. S. and Do, D. D., "A Unique Behavior of Sub-critical Hydrocarbon Permeability in Activated Carbon at Low Pressures," *Korean J. Chem. Eng.*, **20**, 1097 (2003).

Bhandarkar, M., Shelekhin, A. B., Dixon, A. G. and Ma, Y. H., "Adsorption, Permeation, and Diffusion of Gases in Microporous Membranes. I. Adsorption of Gases on Microporous Glass Membranes," *J. Memb. Sci.*, **75**, 221 (1992).

Bhave, R. R., "Inorganic Membranes: Synthesis, Characteristics and Applications," Van Nostrand Reinhold, New York (1991).

Bond, R. L., ed., "Porous Carbon Solids," New York, Academic Press, Chaps. 1,5 and 6 (1967).

Burggraaf, A. J. and Cot, L., "Fundamentals of Inorganic Membrane Science and Technology," Elsevier (1996).

Hasegawa, Y., Tanaka, T. and Watanabe, K., "Separation of CO_2-CH_4 and CO_2-N_2 System Using Ion-exchange FAU-Zeolite Membrane with Different Si/Al Ratios," *Korean J. Chem. Eng.*, **19**, 309 (2002).

Hwang, S. T. and Kammermeyer, K., "Membranes in Separations," John Wiley & Son (1975).

Jia, M. D., Baoshu, B., Noble, R. D. and Falconer, J. L., "Ceramic-zeolite Composite Membranes and their Application for Separation of Vapor/Gas Mixtures," *J. Memb. Sci.*, **90**, 1 (1994).

Jolinde, M., van de Graaf, Kapteijn, F. and Moulijn, J. A., "Diffusivities of Light Alkanes in a Silicalite-1 Membrane Layer," *Microporous and Mesoporous Materials*, **35-36**, 267 (2000).

Jolinde, M., van de Graaf, Kapteijn, F., Jacob, A. and Moulijn, J. A., "Methodological and Operational Aspects of Permeation Measurements on Silicalite-1 Membranes," *J. Memb. Sci.*, **144**, 87 (1998).

Kapoor, A., Yang, R. T. and Wong, C., "Surface Diffusion," *Catal. Rev., Sci. Eng.*, **31**, 129 (1989).

Karger, J. and Ruthven, D. M., "Diffusion in Zeolites and other Microporous Solids," John Wiley & Sons (1992).

Keizer, K., Uhlhorn, R. J. R., Van Vuren, R. J. and Burggraaf, A. J., "Gas Separation Mechanisms in Microporous Modified γ-Al_2O_3 Membranes," *J. Memb. Sci.*, **39**, 285 (1988).

Kim, S. S. and Sea, B. K., "Gas Permeation Characteristics of Silica/Alumina Composite Membrane Prepared by Chemical Vapor Deposition," *Korean J. Chem. Eng.*, **18**, 322 (2001).

Kim, Y. S., Kusakabe, K. and Morooka, S., "Preparation of Microporous Silica Membranes for Gas Separation," *Korean J. Chem. Eng.*, **18**, 106 (2001).

Lee, D. and Oyama, S. T., "Gas Permeation Characteristics of a Hydrogen Selective Supported Silica Membrane," *J. Memb. Sci.*, **210**, 291

(2002).
Raman, N. K. and Brinker, C. J., "Organic Template Approach to Molecular Sieving Silica Membranes," *J. Memb. Sci.*, **105**(3), 273 (1995).
Rao, M. B. and Sircar, S., "Nanoporous Carbon Membranes for Separation of Gas Mixtures by Selective Surface Flow," *J. Memb. Sci.*, **85**, 253 (1993).
Ross, S. and Oliver, J. P., "On Physical Adsorption," Interscience, New York (1964).
Talu, O. and Kabe, R. L., "Isosteric Heat of Adsorption and the Vacancy Solution Model," *AIChE J.*, **33**, 510 (1987).
Uchytil, P., "Gas Permeation in Ceramic Membranes Part 1. Theory and Testing of Ceramic Membranes," *J. Memb. Sci.*, **97**, 139 (1994).
Vroon, Z. A. E. P., Keizer, K., Gilde, M. J., Verweij, H. and Burggraaf, A. J., "Transport Properties of Alkanes through Ceramic Thin Zeolite MFI Membranes," *J. Memb. Sci.*, **113**, 293 (1994).
West, G. D., Diamond, G. G., Holland, D., Smith, M. E. and Lewis, M. H., "Gas Transport Mechanisms through Sol-gel Derived Templated Membranes," *J. Memb. Sci.*, **203**, 53 (2002).
Xomeritakis, G., Naik, S., Braunbarth, C. M., Cornelius, C. J., Pardey, R. and Brinker, C. J., "Organic-templated Silica Membranes: I. Gas and Vapor Transport Properties," *J. Memb. Sci.*, **215**, 225 (2003).
Yang, R. T., "Gas Separation by Adsorption Processes," Butterworths (1987).
Yang, S. M., Lee, Y. E., Hyun, S. H. and Lee, C. H., "Organic-Templating Approach to Synthesis of Nanoporous Silica Composite Membranes (I): TPA-Templating and CO_2 Separation," *J. Materials Sci.*, **37**, 1 (2002).